Fluidization of fine calciner raw meal particles by mixing with coarser inert particles – Experiments and CPFD simulations

Ron M Jacob Britt M.E. Moldestad Lars-Andre Tokheim

Department of Process, Energy and Environmental Technology, University of South-Eastern Norway
{ron.jacob, britt.moldestad, Lars.A.Tokheim}@usn.no

Abstract

The calciner has a significant role in the production of cement. It is the most energy-intensive process unit in the production process. Most modern calciners are entrainment-based, i.e., a hot gas pneumatically conveys the particles through the calciner. A fluidized bed is an alternative to the entrainment calciner, which may be of special interest if the calcination process is to be electrified, so that the raw meal is mainly calcined by heat transfer from a hot surface and not by direct contact with hot combustion gases. The fine particle size of the raw meal, however, makes it a challenge to fluidize. This study looks into an alternative solution in which the cement raw meal is mixed with coarse sand particles to enhance the fluidization behavior.

Experiments are first conducted to fluidize pure cement raw meal (fine particles) and sand (coarse particles) separately. Then they are mixed at fine/coarse mass ratios of 25%/75% and 50%/50%.

Simulations are then performed, using a commercial CPFD software (Barracuda ®, version 20.0.0), to replicate the results from the experiments.

The experimental results indicate that it is technically feasible to fluidize cement raw meal by mixing it with coarse inert particles at the mentioned fine/coarse mass ratios. Stable fluidization was observed at a superficial gas velocity of 0.3 m/s. The pressure drop results from simulations and experiments matched quite well at both mixing ratios. Hence, the CPFD simulations may be used as an aid in the design of a potential full-scale calciner applying this concept.

Keywords: Fluidization, Cement, Binary particles, Calcination, Electrification

1 Introduction

Around 7% of the global CO_2 emissions are from the cement industry (IEA, 2020). In modern cement plants, the CO_2 comes from the decarbonation of the calcium carbonate in the raw meal (about 70 %) and from the fuel combustion (about 30 %). Reducing the CO_2 emissions from such plants can be done by post-combustion capture of the CO_2 in the exhaust gas from the plant. However, calcination by electrification of the calciner will generate a pure gas CO_2, which makes it possible to significantly reduce the CO_2 emissions without building a separate capture plant, provided the electricity is produced from a renewable energy source. This method can reduce around 70 % of the CO_2 emissions from a modern cement plant (Tokheim *et al.*, 2019).

Most modern calciners operate in the entrainment mode where the raw meal is entrained by the combustion flue gases while providing heat for calcination reaction (Becker *et al.*, 2016). It may be possible to electrify the entrainment calciner by inserting heating rods. However, the main challenge with this concept is the potential heat loss from a large amount of recycling gas required for raw meal entrainment (Jacob and Tokheim, 2021).

An alternative solution to this concept is a fluidized bed calciner, which will operate at a lower velocity and will require much less recycle gas. Moreover, a high heat transfer coefficient and a uniform temperature distribution due to good mixing in the system are additional advantages (Kunii and Levenspiel, 1991). However, due to the small particle size in a traditional cement raw meal, it may not be feasible to fluidize the particles properly (Samani, 2020).

A raw meal typically has a particle size distribution in the range 0.5 – 250 µm, where 70-80% of the particles fall in the range of the Geldart C particle size class. Geldart C particles are difficult to fluidize due to their cohesive nature (Geldart, 1973). A previous investigation demonstrated this challenge as rat hole formation in the bed was observed (Samani *et al.*, 2020).

Mixing the cement raw meal with coarse particles could be an alternative way of fluidizing these particles (Samani *et al.*, 2020). This concept of mixing cement raw meal with coarse inert particles is called "Powder-Particle Fluidized Bed (PPFB)" (Kato *et al.*, 1991). The PPFB concept was demonstrated experimentally at a limestone feeding rate of 15 g/hr and a superficial gas velocity of 0.45 m/s. The static bed height of coarse particles was varied in the range 0.1 – 0.2 m. The experiment was done in a column with a diameter of 0.03 m and a height of 0.65 m (Tashimo *et al.*, 1999).

This study aims to investigate the feasibility of fluidizing a binary mixture by mixing fine cement raw meal and coarse sand particles at a mass ratio that may be appropriate for a full-scale process. The feasibility is tested experimentally with a cold-flow lab-scale fluidized bed at different mass ratios. Computational particle and fluid dynamics (CPFD) simulations are

further performed with the commercial software Barracuda ®, version 20.0.0, to check if the results from the experiments can be replicated through computer simulations. The intention is to use the results from this study to design a full-scale calciner.

2 Experimental Method

The experimental setup, the particle characteristics, and the experimental procedure are described below.

2.1 Experimental setup

The experiments were conducted in a lab-scale fluidized bed. The lab-scale fluidized bed is a cylindrical tube made of Lexan plastic. The internal diameter and the height of the tube are 0.085 and 1.4 m, respectively. The tube has nine pressure transmitters placed along its axial direction, and a LabVIEW® programme records the pressure readings. The experimental setup is shown in Figure 1.

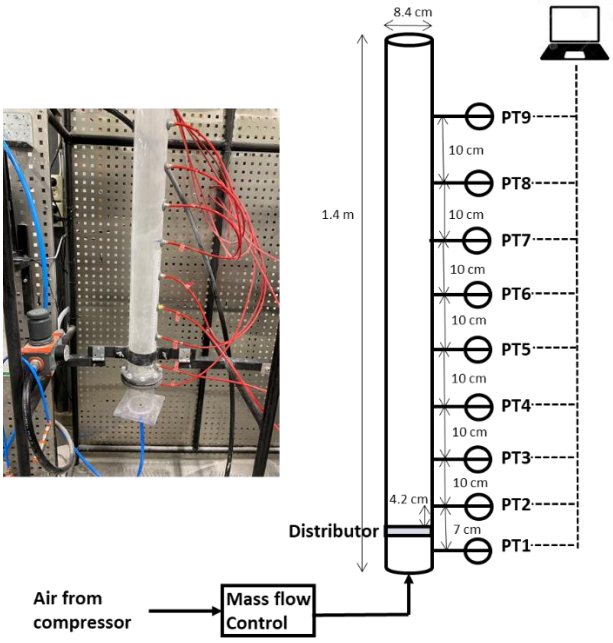

Figure 1: Experimental setup

The distance between PT1 and PT2 is 7 cm, and the other transmitters have an equal spacing of 10 cm, as shown in Figure 1. The particles are fluidized with air at ambient conditions. The mass flow rate of the air is controlled with a flowmeter.

The air distributor, made of a highly porous sintered stainless steel (Siperm R20®, Tridelta Siperm GmbH), is placed between the fluidizing air and particles. The porosity of the distributor is 37-42 %.

The pressure drop from the air distributor (ΔP_d) was measured at different gas velocities by passing air through the distributor without any presence of particles. The pressure drop versus air velocity was then fitted to a non-linear equation. The experimental result of pressure drop and the prediction from the non-linear equation are shown in Figure 2.

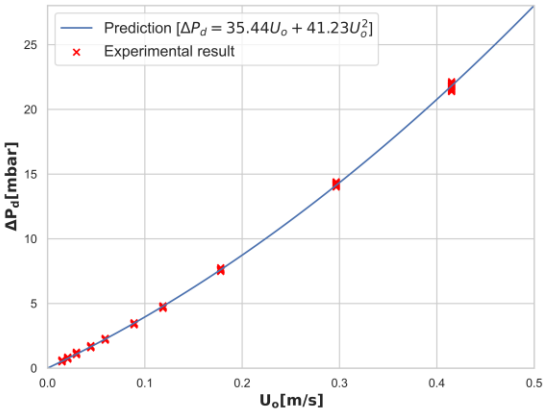

Figure 2: Fitting pressure drop across the distributor to second order velocity function.

2.2 Particle characteristics

A regular cement raw meal from a local Norwegian cement plant was used as fines in the experiment. The fine particles had a size distribution between 0.5 and 250 µm, and almost 80 % of the particles were below 30 µm. Sand with a particle size between 100 and 600 µm was used as the coarse particles in the experiment.

Four different mass fractions of fines were used in the experiments; 0, 25, 50 and 100 %. The total mass of fine and coarse particles was 900 g in all experimental cases. An overview of the experimental cases and the particle properties is shown in Table 1.

Table 1: Experimental cases and particle properties

Parameters	100% fines	50% fines	25% fines	0% fines
Mass of raw meal [kg]	0.9	0.45	0.225	0
Mass of sand [kg]	0	0.45	0.675	0.9
Average particle density [kg/m³]	2897	2774	2712	2650
Bed Height [cm]	15.2	11.7	10.4	10.2
Bulk density [kg/m³]	1053	1368	1540	1570
Void fraction [-]	0.64	0.51	0.43	0.41

Laser diffraction with a HELOS (RODOS dry dispersion) particle size analyzer was used to measure the particle size distribution (PSD) for each case. The resulting distribution is shown in Figure 3.

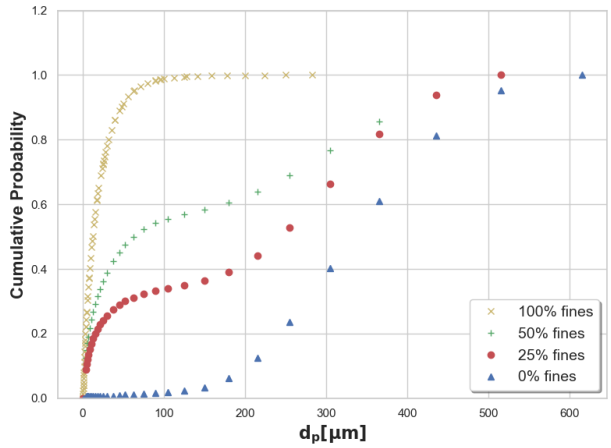

Figure 3: Cumulative particle size distribution (PSD) plot for the experimental cases

2.3 Experimental procedure

The particles were carefully weighed and poured into the column. The bed height in each case was noted down (cf. Table 1).

The air velocity was then increased in steps to different levels. By experience it was found that the system reached a pseudo-steady state within 160 seconds at a certain level. Hence, for each step, the velocity was held constant for 200 seconds. The pressure measurements between 160 and 200 s were used to determine the mean pressure and pressure fluctuations at the pseudo-steady state conditions. A high standard deviation in these fluctuations may indicate a bubbling behavior in the bed (Jaiswal *et al.*, 2018).

3 Modelling methods

Monte-Carlo simulations were used to numerically determine the PSD of the mixtures. Computational particle and fluid dynamics (CPFD) modelling was used to simulate the particle behaviour in the bed, applying a suitable drag model. These models, as well as the simulation setup, are described below.

3.1 Monte-Carlo simulations to analyze PSD

A Monte-Carlo simulation may be used to analyze the particle size distribution (PSD). According to the law of large numbers, as the sample size increases, the distribution of the sampled particles tends to have its original distribution. Samples may be generated from the distribution using various algorithms. In this study, a modified version of the inverse sampling algorithm is used:

1. Generate a random number between 0 and 1 from a uniform distribution. This number represents the cumulative probability (y-axis) in Figure 3.
2. At the randomly generated cumulative probability, read the value of diameter (d_p) by linear interpolation. This value of d_p is the generated sample.
3. Repeat step 1 and step 2 to get the required number of samples (10,000 in our case).

The histogram of the generated sample may, however, not be smooth enough to make inferences. Kernel density estimation (KDE) is a non-parametric method to estimate the probability density from random variates. It is used for data smoothening where inferences about the data must be made. The KDE algorithm implemented in the Seaborn package of Python 3.8 was used to smoothen the distribution. This method is useful for predicting the probability density of the mixture if the probability density of pure components is known. The prediction test is also simulated in this study.

3.2 CPFD method

Computational particle and fluid dynamics (CPFD) is a method to simulate gas-solids multiphase flow. This method is based on Eulerian-Lagrangian coupling, and it uses a unique concept called the multiphase-particle-in-cell (MP-PIC) method (Andrews and O'Rourke, 1996). The MP-PIC method solves the gas phase equation by the Eulerian approach and the solid phase equations by the Lagrangian approach. This approach makes it quite similar to the traditional discrete element method (DEM). However, some differences, such as the particle-to-particle force calculations and the assumption of numerical particles, make the CPFD method much more computationally efficient than the traditional DEM method for an industrial system (Snider, 2007).

The simulations were performed at the experimental conditions to study the physics of particles in each case.

The volume-averaged continuity and momentum equation for a two-phase incompressible flow is (Snider 2007),

$$\frac{\delta \theta_f}{\delta t} + \nabla \cdot \left(\theta_f u_f\right) = 0 \tag{1}$$

$$\frac{\delta \left(\theta_f u_f\right)}{\delta t} + \nabla \cdot \left(\theta_f u_f u_f\right) = \frac{-1}{\rho_f}\nabla p - \frac{1}{\rho_f} F + \theta_f g + \frac{1}{\rho_f}\nabla \cdot \tau \tag{2}$$

Here, θ_f is the fluid volume fraction, u_f is the fluid velocity, ρ_f is the fluid density, p is the fluid pressure, τ is the fluid stress tensor, g is the gravitational constant, and F is the momentum exchange rate per volume between fluid and the particles.

The acceleration in the particles can be further modelled by (Snider, 2007),

$$\frac{\delta u_p}{\delta t} = D(u_f - u_p) - \frac{1}{\rho_p}\nabla p + g - \frac{1}{\theta_p \rho_p}\nabla \tau_p + F_S \quad (3)$$

Here, u_p is the particle velocity, ρ_p is particle density, D is the interphase drag function, θ_p is the particle void fraction, τ_p is the particle normal stress and F_S is the particle friction.

The particle-to-particle forces are modelled with the normal stress of particle (τ_p), and this is given by (Snider 2001),

$$\tau_p = \frac{P_s {\theta_p}^{\beta}}{max[\theta_{cp} - \theta_p, \varepsilon(1 - \theta_p)]} \quad (4)$$

Here the constant P_s has a unit of pressure, θ_{cp} is particle void fraction at close packing, β is a constant with a recommended value between 2 and 5, ε is a very small number activated when particle void fraction comes very close to its close pack limit.

The blended acceleration model (BAM) is an extra option implemented in Barracuda to account for the fluidization behavior of particles of different size. The particles with different size have a lower relative motion due to sustained particle contacts. BAM is used to simulate this phenomenon, and without BAM, the segregation of particles in simulations may be higher than in reality.

Particle to wall interaction modelling in Barracuda is controlled mainly by three variables; normal-to-wall momentum retention (r_N), tangent-to-wall momentum retention (r_T) and diffuse bounce index (d_{bi}).

A schematic of a particle colliding with a wall with initial velocity (u^n) and attaining a final velocity (u^{n+1}) is shown in Figure 4.

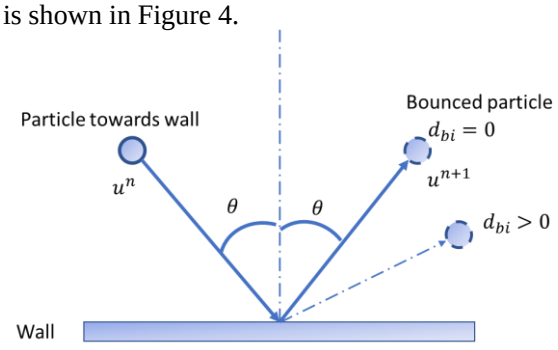

Figure 4: Schematic of particle collision with the wall

The diffuse bounce index (d_{bi}) defines the degree of scattering of particles after the collision (cf. Figure 4). This parameter applies to a rough wall, which is usually present in an industrial system. The normal-to-wall momentum retention (r_N) is the fraction of the normal component of particle momentum retained after a collision with wall. The tangent-to-wall momentum retention (r_T) is the fraction of tangential component of particle momentum retained after a collision with wall.

The choice of values for the parameters discussed in this section varies in the literature. The values used in this study are shown in Table 2.

Table 2: Particle interaction parameters used in this study

Particle-to-particle interaction		Particle-to-wall interaction	
Parameter	**Value**	**Parameter**	**Value**
$\boldsymbol{P_s}$	1	r_N	0.4
$\boldsymbol{\beta}$	3	r_T	0.95
$\boldsymbol{\varepsilon}$	10^{-8}	d_{bi}	2

3.3 Drag modelling

The interphase drag function (D) is used to model particle acceleration. There are many models available for drag modelling.

The Ergun drag model defines this function as (Beetstra *et al.*, 2007),

$$D = 0.5\left(\frac{c_1 \theta_p}{\theta_f Re} + c_o\right)\frac{\rho_f(u_f - u_p)}{r_p \rho_p} \quad (5)$$

Here, c_o and c_1 are model coefficients and recommended value for c_o is 2 and for c_1 is 180 (Beetstra *et al.*, 2007). This model was developed using data for a dense bed.

The Wen-Yu drag model was developed based on fluid void fraction and single-particle drag (Wen and Yu, 1966). The drag coefficient is defined as,

$$C_d = \begin{cases} \frac{24}{Re}{\theta_f}^{n_o} & Re < 0.5 \\ \frac{24}{Re}{\theta_f}^{n_o}(c_o + c_1 Re^{n_1}) & 0.5 \le Re \le 1000 \\ c_2 {\theta_f}^{n_o} & Re > 1000 \end{cases} \quad (6)$$

Here, the drag coefficient (C_d) is related to the interphase drag function by,

$$D = \frac{3}{8} C_d \frac{\rho_f(u_f - u_p)}{r_p \rho_p} \quad (7)$$

The Wen-Yu drag model is more appropriate for dilute flows, while the Ergun drag model is more appropriate for dense flows. Using a blend may capture the best of both drag models. The blended model is given by,

$$D = \begin{cases} D_1 & \theta_p < 0.75\theta_{CP} \\ \frac{(D_2 - D_1)(\theta_p - 0.75\,\theta_{cp})}{0.85\theta_{cp} - 0.75\theta_{cp}} + D_1 & 0.75\theta_{cp} \le \theta_p \le 0.85\theta_{cp} \\ D_2 & \theta_p > 0.85\theta_{CP} \end{cases} \quad (8)$$

Here, D_1 is the drag function from the Wen-Yu equation and D_2 is the drag function from the Ergun equation.

In this study, the blended model was used for the coarse particles and the mixture cases, whereas the Wen-Yu model was used for the fine cement raw meal.

3.4 Simulation setup

The simulations were set up to match the experimental conditions. A three-dimensional geometry of the tube

was developed with an internal diameter of 0.085 and a height of 1.4 m. A uniform grid with a total of 17600 (10×10×176) cells in the tube was created. The pressure sensors were placed at the height of 4.2 cm and 14.2 from the bottom to replicate the PT2 and PT3 sensors. The resulting mesh and the pressure monitoring points are shown in Figure 5.

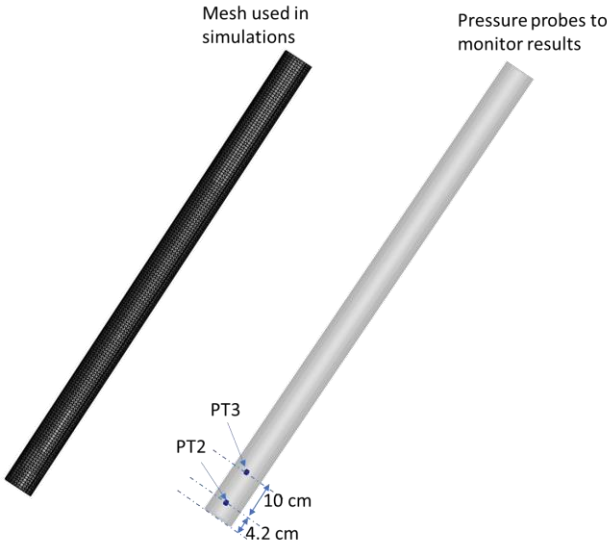

Figure 5: Mesh used in the simulations and pressure probe to monitor results

The simulation results are presented after simulating for 30 seconds in each case as it was found that a pseudo-steady state was reached after 30 seconds of simulations.

4 Results and Discussions

4.1 Monte-Carlo simulation results

The PSDs from the Monte-Carlo simulations are given in Figure 6. Results from mixing pure particles are given in Figure 7. The results indicate that Monte-Carlo sampling is an efficient algorithm to estimate the particle size distribution of mixed powders.

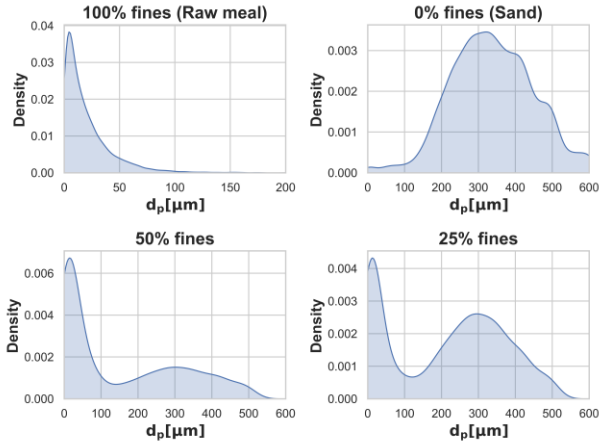

Figure 6: Probability distribution of the particles

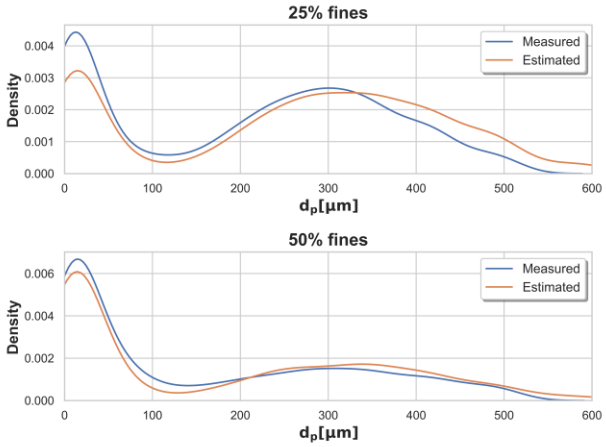

Figure 7: Sampling from measured PSD vs estimated PSD by sampling from pure powders

4.2 Pure particle results

A corrected pressure drop between PT1 and PT2 (cf. Figure 1) was calculated by subtracting the pressure drop over the distributor from the measured pressure drop between point 1 and 2 (cf. Figure 2). The corrected bed pressure drop between PT1 and PT2 (excluding distributor pressure drop), ΔP_{12}, is shown in Figure 8. The standard deviation of the pressure drop (σ_P) is plotted as a band and also as a separate dotted line.

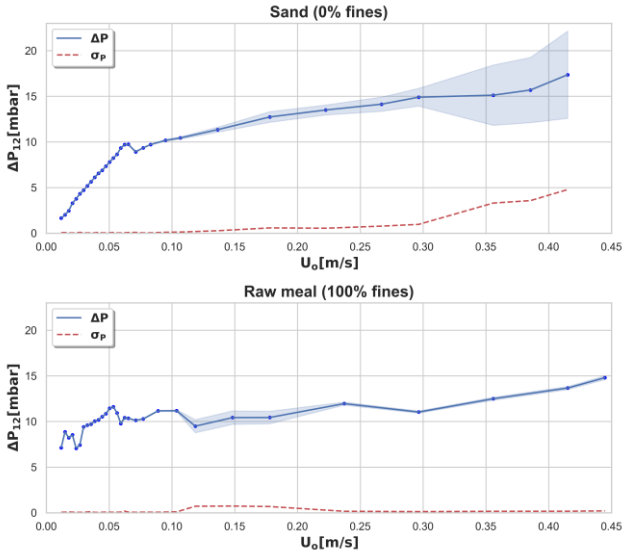

Figure 8: Pressure drop profile for pure particle fluidization

The minimum fluidization velocity (U_{mf}) for the pure coarse particles is at a superficial gas velocity of 0.06 m/s. The minimum fluidizing velocity (U_{mf}) of the fine particles could not be measured accurately as the disturbances in the bed started at the lowest superficial gas velocity of 0.01 m/s. Both coarse and fine particles had similar pressure drop readings at the fluidizing conditions because the weight of both particles is the same. The pressure drop fluctuations for coarse particles are high when the velocity is high. In contrast, for the

fine cement raw meal, the fluctuations were low. These results indicate an excellent fluidization behavior of the sand particles and poor fluidization behavior of the fine cement raw meal. This inference is also consistent with visual observation of the bed.

The corrected bed pressure drop between PT1 and PT2 (excluding distributor pressure drop), ΔP_{12}, is not directly comparable to the simulation results as pressure point 1 in the experiment is not present in the simulation model. So, the experimental pressure drop between sensor PT2 and PT3 (ΔP_{23}) is compared against the simulation results for pure particles in Figure 9.

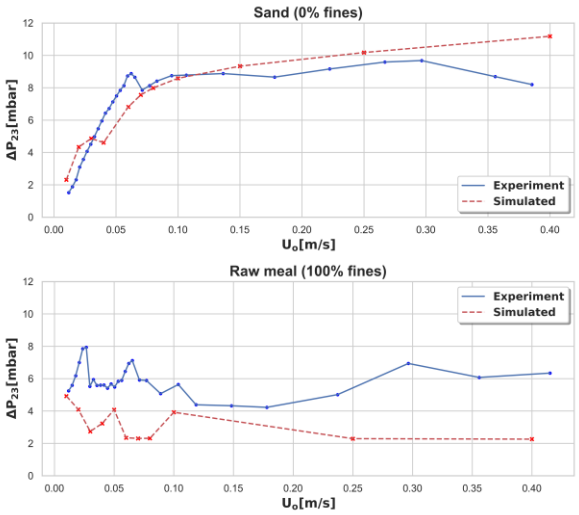

Figure 9: Pressure drop profile comparison of experiments and simulations for pure particles

The results for the coarse particles show that the measured and simulated pressure drop match quite well. In the experiments, a pressure drop peak corresponding to the minimum fluidization velocity is observed. In the simulation, however, the peak is predicted at a lower velocity. This peak may not be the minimum fluidization velocity as the pressure drop keeps increasing almost at the same gradient after the peak. The simulated pressure drop curve starts to flatten out at a velocity higher than the minimum fluidization velocity predicted from experiment. Thus, the minimum fluidization velocity value predicted from the simulation is higher than the experimental value. The coarse particles have a wide size distribution (cf. Figure 3), which means an interaction between particles of different sizes is expected. Some of the interaction effects are neglected in the CPFD model and could be a reason for the deviation. This effect may be modelled with the BAM feature (cf. Section 3.2). However, for this work, the current results are considered good enough for further analysis.

The results for the fine particles show that the pressure drop is under-predicted in all the cases. In a real system, the particles tend to agglomerate, and this increases the pressure drop in the system. This agglomeration effect may be the reason for the deviation as it is not modelled in this study. Still, the results are considered good enough for further study.

4.3 Experimental results of binary particle

The pressure drop (ΔP_{12}) results from fluidizing binary particles were estimated in the same way as in Section 4.2. The results are shown in Figure 10.

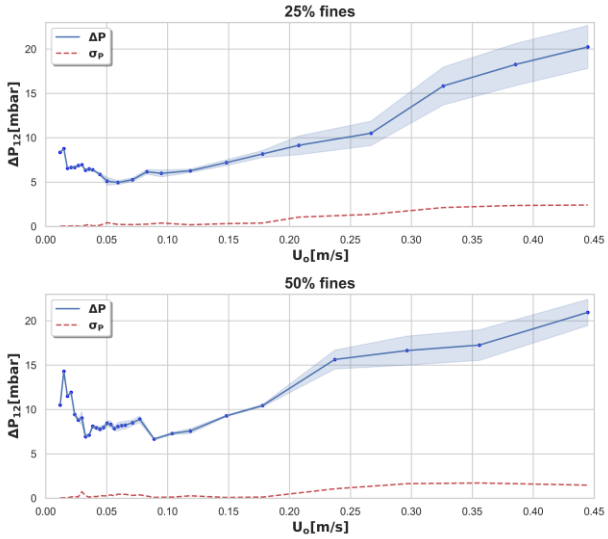

Figure 10: Pressure drop profile for mixed particles

The minimum fluidizing velocity (U_{mf}) could not be accurately determined as the disturbances started at the lowest velocity (0.01 m/s) in both cases of binary particle fluidization. A low minimum fluidizing velocity for a binary mixture may be expected for a large particle size ratio (Rao and Curtis, 2011). A large particle size ratio is present in this study, as the Sauter mean diameter of the fine cement raw meal is 5µm and that for the coarse sand is 226 µm. Sharp peaks in the pressure drop are observed when the binary particles are fluidized. One explanation for the sharp peaks is the phenomenon of entrapment. According to this phenomenon, if some of the fine particles in the top layer are entrapped by the coarse particles, at a sufficiently high gas velocity, the fines may gain enough momentum to break through the bed, causing pressure drop peaks (Rao and Curtis, 2011).

The primary outcome of this study is the fluidization conditions of the binary particles. The pressure drop fluctuations had a relatively high standard deviation in both cases of binary mixing. This observation may indicate good bubbling behavior. However, the visual observation showed a better bubbling behavior for the case with a 25%/75% fine/coarse mass ratio. This mixing ratio may be good for operating the fluidized bed calciner. However, additional studies on the segregation pattern should be done to determine if the fine cement raw meal particles may be removed easily from the binary mixture.

4.4 Simulation of binary particles

A comparison of pressure drop readings in experiments and simulations is shown in Figure 11.

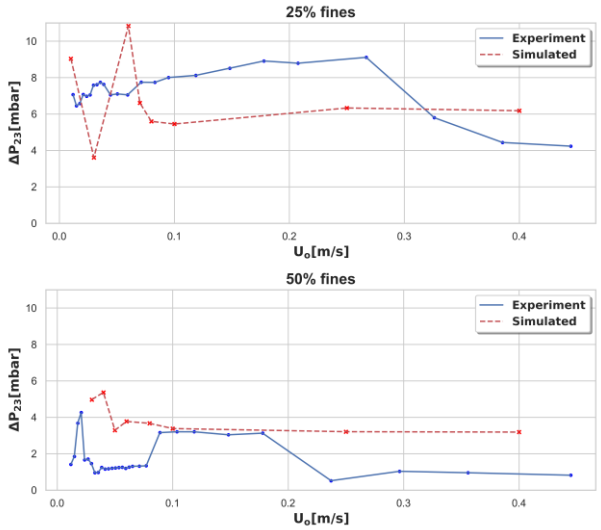

Figure 11: Pressure drop profile comparison of experiment and simulations for mixed particles

The deviations in the pressure drop profile may be due to the deviations in the pure component (discussed in Section 4.2). Additional deviations may be due to segregation effects in the mixed state. However, the pressure drop results are in the same range. Thus, the results may be useful for additional simulations of a full-scale calciner.

Simulation results are shown in Figure 12 and Figure 13. The results are displayed at different superficial gas velocities (U_o) after 30 seconds of simulation (system reached a pseudo-steady state). The fine particles are displayed in green color and coarse particles are displayed in red color.

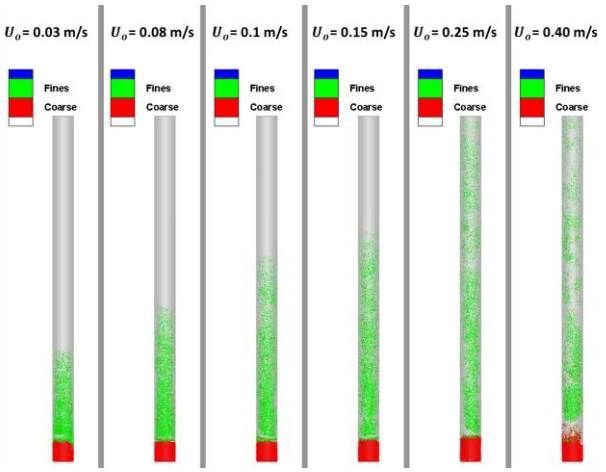

Figure 12: Simulation results from 25% fines at different superficial gas velocities (U_o) (Green = Fines, Red = Coarse)

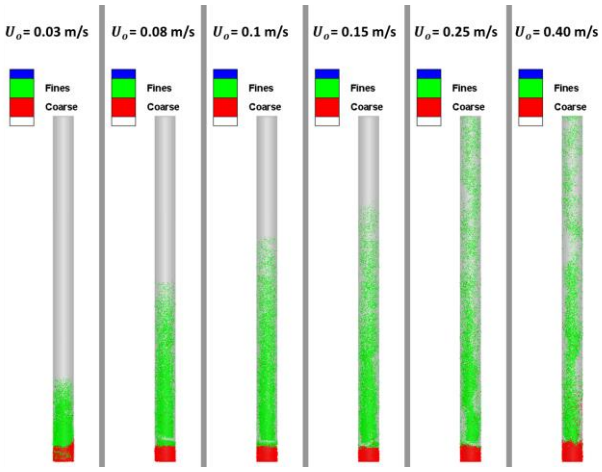

Figure 13: Simulation results from 50% fines at different superficial gas velocities (U_o) (Green = Fines, Red = Coarse)

The snapshots of simulation results shows that the fine particle rises in the column as the superficial gas velocity is increased. At superficial gas velocity of around 0.25 m/s, the fine particles are entrained up to the total column length. The fine particles are further entrained outside the column at this gas velocity. These results may be useful while designing a full-scale calciner.

5 Conclusion

Fluidizing fine cement raw meal (fines) by mixing with sand (coarse) particles appears to be technically feasible. The standard deviation of the pressure fluctuation is a good measure to determine the fluidization conditions. The pure coarse particles had the best fluidizing quality, as expected, while the pure fine particles did not fluidize. For the binary mixtures, stable fluidization was observed with a superficial gas velocity higher than 0.25 m/s at fine/coarse mass ratios of 25%/75% and 50%/50%.

Visually, the fluidization quality was better with a fine/coarse mass ratio of 25%/75%. This condition may be used to operate a fluidized bed calciner by mixing cement raw meal and inert coarse particles.

Simulations were performed to replicate the results from the experiments. The results showed some deviations in pressure drop predictions. However, results were not too far off, so simulations may be applied to a scaled-up version of the calciner.

In practice, some other factors such as segregation, separation efficiency, effect on capacity and energy with 25 % fines, should be addressed in further studies. Considering these effects, an appropriate height should be selected to remove the fines from the top of the bed. Alternatively, a classifier (Jayarathna et. al., 2019) may be placed downstream to separate the fines and the coarse particles. These factors may be included in later studies of a scaled-up version of the calciner.

Acknowledgements

This study was carried out as part of the research project "Combined calcination and CO_2 capture in cement clinker production by use of CO_2-neutral electrical energy – Phase 2". Gassnova and Norcem are greatly acknowledged for funding this project.

References

M. J. Andrews, P. J. O'Rourke. The multiphase particle-in-cell (MP-PIC) method for dense particulate flows. *Int. J. Multiphase Flow*, Vol. 22, No. 2, pp. 379-402, 1996

Simon Becker, Robert Mathai, Kristina Fleiger, Giovanni Cinti. Status report on calciner technology. *CEMCAP*, Rev. 2, 2016.

R. Beetstra, M. A. van der Hoef, J. A. M. Kuipers. Drag force of intermediate Reynolds number flow pas mono- and bidisperse arrays of spheres. *AIChE Journal*, Vol. 53, 2007.

D. Geldart. Types of gas fluidization. *Powder Technology*, Vol 7, pp. 285-292, 1973.

IEA, Technology Roadmap - Low-Carbon Transition in the Cement Industry. 2018.

Ron M. Jacob, Lars-André Tokheim. Electrification of an entrainment calciner in a cement kiln system – heat transfer modelling and simulations. Submitted to the *SIMS conference*, 2021.

Rajan Jaiswal, Cornelius E. Agu, Rajan K. Thapa, Britt M. E. Moldestad. Study of fluidized bed regimes using computational particle fluid dynamics. *SIMS*, 59, 2018.

Chameera K. Jayarathna, Michael Balfe, Britt M.E. Moldestad, Lars-Andre Tokheim. Improved multi-stage cross-flow fluidized bed classifier. *Powder Technology*, Vol 342, pp. 621-629, 2019.

K. Kato, T. Takarada, N. Matsuo, T. Suto, N. Nakagawa. Residence time distribution of fine particles in a powder-particle fluidized bed. Kagaku Kogaku Ronbunshu, Vol. 17, pp. 970-975, 1991.

Daizo Kunii, Octave Levenspiel. Fluidization Engineering, *Butterworth-Heinemann series in chemical engineering*, Edition 2, 1991.

Akhil Rao, Jennifer S. Curtis. Classifying the fluidization and segregation behavior of binary mixtures using particle size and density ratios. *AIChE Journal*, Vol. 57, No. 6, 2011.

Nastaran Ahmadpour Samani. Calcination in an electrically heated bubbling fluidized bed applied in calcium looping, *Master's thesis*, USN, 2020.

Dale M. Snider. An incompressible three-dimensional multiphase particle-in-cell model for dense particle flows. *Journal of Computational Physics*. 170, pp. 523-549, 2001

Dale M. Snider. Three fundamental granular flow experiments and CPFD predictions, *Powder Technology*, Vol. 176, pp. 36-46, 2007.

Tsutomu Tashimo, Tomohiko Suto, Jun Murota, Kunio Kato. Calcination of fine limestone particles by a powder particle fluidized bed. *Journal of chemical engineering of Japan*, Vol. 32, pp. 374-378, 1999.

Lars-André Tokheim, Anette Mathisen, A., Lars E. Øi, Chameera Jayarathna, Nils H. Eldrup and Tor Gautestad. Combined calcination and CO_2 capture in cement clinker production by use of electrical energy, SINTEF proceedings, 4, pp 101-109, 2019

C. Y. Wen, Y. H. Yu. Mechanics of fluidization. Chemical Engineering Process Symposium, pp. 100-111, 1966.